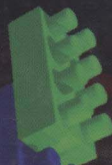
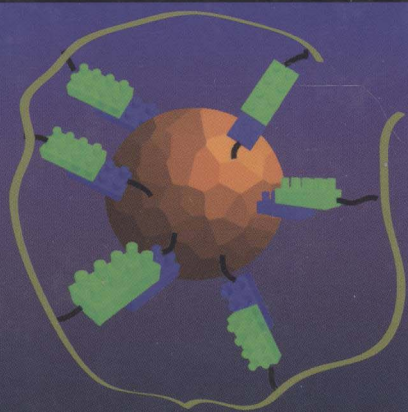


# Molecular Recognition and Polymers

*Control of Polymer Structure and Self-Assembly*

*Edited by*

*Vincent Rotello and S. Thayumanavan*



063  
M718

---

# MOLECULAR RECOGNITION AND POLYMERS

Control of Polymer Structure and  
Self-Assembly

---

Edited by

VINCENT M. ROTELLO

S. THAYUMANAVAN



E2009000121

A JOHN WILEY & SONS, INC., PUBLICATION

Copyright © 2008 by John Wiley & Sons, Inc. All rights reserved

Published by John Wiley & Sons, Inc., Hoboken, New Jersey.

Published simultaneously in Canada

No part of this publication may be reproduced, stored in a retrieval system, or transmitted in any form or by any means, electronic, mechanical, photocopying, recording, scanning, or otherwise, except as permitted under Section 107 or 108 of the 1976 United States Copyright Act, without either the prior written permission of the Publisher, or authorization through payment of the appropriate per-copy fee to the Copyright Clearance Center, Inc., 222 Rosewood Drive, Danvers, MA 01923, (978) 750-8400, fax (978) 750-4470, or on the web at [www.copyright.com](http://www.copyright.com). Requests to the Publisher for permission should be addressed to the Permissions Department, John Wiley & Sons, Inc., 111 River Street, Hoboken, NJ 07030, (201) 748-6011, fax (201) 748-6008, or online at <http://www.wiley.com/go/permission>.

**Limit of Liability/Disclaimer of Warranty:** While the publisher and author have used their best efforts in preparing this book, they make no representations or warranties with respect to the accuracy or completeness of the contents of this book and specifically disclaim any implied warranties of merchantability or fitness for a particular purpose. No warranty may be created or extended by sales representatives or written sales materials. The advice and strategies contained herein may not be suitable for your situation. You should consult with a professional where appropriate. Neither the publisher nor author shall be liable for any loss of profit or any other commercial damages, including but not limited to special, incidental, consequential, or other damages.

For general information on our other products and services or for technical support, please contact our Customer Care Department within the United States at (800) 762-2974, outside the United States at (317) 572-3993 or fax (317) 572-4002.

Wiley also publishes its books in a variety of electronic formats. Some content that appears in print may not be available in electronic formats. For more information about Wiley products, visit our web site at [www.wiley.com](http://www.wiley.com).

***Library of Congress Cataloging-in-Publication Data:***

Molecular recognition and polymers: control of polymer structure and self-assembly / [edited by] Vincent Rotello, Sankaran Thayumanavan.  
p. cm.

Includes index.

ISBN 978-0-470-27738-6 (cloth)

1. Biomimetic polymers. 2. Molecular recognition. 3. Supramolecular chemistry.

I. Rotello, Vincent M. II. Thayumanavan, Sankaran.

QD382.B47M65 2008

547'.1226-dc22

2008007590

Printed in the United States of America

10 9 8 7 6 5 4 3 2 1

# MOLECULAR RECOGNITION AND POLYMERS

This book is dedicated to the memory of Dmitry Rudkevich, and to his wife,  
Sasha, and sons, Dmitry Jr. and Eric.

# PREFACE

---

Inter- and intramolecular networks of non-covalent interactions are responsible for a wide array of phenomena in fields of biology and chemistry. Biological systems use specific patterns of complementary functionality to provide exquisite control over biopolymer recognition processes such as protein–protein and protein–polynucleic acid binding. In Nature, these specific supramolecular interactions play many key roles, including stabilization of structure, information storage and transfer, catalysis and self-assembly. Likewise, controlled application of non-covalent interactions provides an effective tool for fabrication of man-made systems, allowing the creation of higher-order architecture required for devices and materials, as well as the dynamic properties required for efficient utilization of these attributes.

The use of specific interactions to control polymer structure and properties is a rapidly emerging field. We have assembled a group of authors at the forefront of this field that are studying both the fundamental science inherent in polymer self-assembly and applications of this strategy to functional systems. This book is designed for researchers in a wide range of areas, and features both fundamental aspects and applications of these fascinating systems.

The book is divided into three sections. The first section provides a general overview of the fundamentals of supramolecular polymers. In Chapter 1, Thibault and Rotello provide a brief introduction to these systems and in Chapter 2, Azagarsamy, Krishnamoorthy, and Thayumanavan describe the rapidly emerging area of amphiphilicity in polymer and dendrimers self-assembly. Interactions at interfaces are sometimes similar but often quite different than those in solution, a topic covered by Loveless, Kersey, and Craig in Chapter 3.

The second section of the book provides a wide variety of examples of the self-assembly of polymer systems. Aspects covered include hydrogen bond-mediated

recognition and self-assembly using block copolymers and telechelic oligomers, as described in Chapter 4 by Mather and Long. Chapter 5 covers the highly versatile “plug and play” non-covalent sidechain modification of polymers, as described by Nair and Weck. Extension of this polymer-mediated assembly to nanoparticles is the focus of Chapter 6 by Chen, Ofir, and Rotello, while Chapter 7 by McKenzie and Rowan describes metallo-supramolecular systems. In Chapter 8, Mason, Steinbacher, and McQuade provide an overview of capsule formation using polymers and biopolymers. Chapter 9 by Gong features the efforts of synthetic chemists to replicate the specific hydrogen bonding patterns found in biology. Chapter 10 focuses on function, with Guan covering the use of supramolecular polymer systems to tailor mechanical properties. Shao and Parquette outline the use of hydrophobicity to control dendrimers structure and dynamics in Chapter 11.

The third section of the book covers the area of biomolecular recognition using polymer systems. The creation of colorimetric sensors using polymers is presented by Basu in Chapter 12. Chapter 13 by Cloninger focuses on glycopolymers and glycodendrimers, while in Chapter 14, Dong, Yuwono, and Hartgerink cover the creation of nanofibers via peptide self-assembly. Finally, in Chapter 15, Wu and Shimizu provide an overview of the field of molecularly-imprinted polymers, describing the formation of these systems and their applications.

Supramolecular chemistry is a beautiful field, featuring modularity, tenability, and versatility. We hope that this book fires your imagination for this emerging field.

VINCENT ROTELLO  
SANKARAN “THAI” THAYUMANAVAN

*Department of Chemistry  
University of Massachusetts, Amherst*

## ACKNOWLEDGMENTS

---

The Editors would like to acknowledge Carol Greene, Denia Fraser, and Denise Schwartz, without whose help this book would not have been possible.



# LIST OF CONTRIBUTORS

---

## Editors

VINCENT M. ROTELLO, Department of Chemistry, Program in Molecular and Cell Biology, University of Massachusetts, Amherst, 710 North Pleasant Street, Amherst, MA 01003, USA

S. THAYUMANAVAN, Department of Chemistry, Program in Molecular and Cell Biology, University of Massachusetts, Amherst, 710 North Pleasant Street, Amherst, MA 01003, USA

## Contributors

MALAR A. AZAGARSAMY, Department of Chemistry, University of Massachusetts, Amherst, 710 North Pleasant Street, Amherst, MA 01003, USA

AMIT BASU, Department of Chemistry, Brown University, Box H, 324 Brook St., Providence, RI 02912, USA

HUNG-TING CHEN, Department of Chemistry, University of Massachusetts, Amherst, 710 North Pleasant Street, Amherst, MA 01003, USA

MARY J. CLONINGER, Department of Chemistry and Biochemistry, Montana State University, 108 Gaines Hall, Bozeman, MT 59717, USA

STEPHEN L. CRAIG, Department of Chemistry, Duke University, Box 90354, Durham, NC 27708-0354, USA

HE DONG, Department of Chemistry, Rice University, Mail Stop 60, 6100 Main Street, Houston, TX 77005

BING GONG, Department of Chemistry, State University of New York, 811 Natural Sciences Complex, Buffalo, NY 14260, USA

ZHIBIN GUAN, Department of Chemistry, University of California, Irvine, 1102 Natural Sciences II, Irvine, CA 92697-2025, USA

JEFFREY D. HARTGERINK, Departments of Chemistry and Bioengineering, Rice University, MS 60, 6100 Main Street, Houston, TX 77005, USA

FARRELL R. KERSEY, Department of Chemistry, Duke University, Box 90354, Durham, NC 27708-0354, USA

K. KRISHNAMOORTHY, Department of Chemistry, University of Massachusetts, Amherst, 710 North Pleasant Street, Amherst, MA 01003, USA

TIMOTHY E. LONG, Department of Chemistry, Macromolecules and Interfaces Institute, Virginia Tech, 107 Davidson Hall, Blacksburg, VA 24061-0001, USA

DAVID M. LOVELESS, Department of Chemistry, Duke University, Box 90354, Durham, NC 27708-0354, USA

BRIAN P. MASON, Baker Laboratory, Department of Chemistry and Chemical Biology, Cornell University, Ithaca, NY 14853, USA

BRIAN D. MATHUR, Hewlett-Packard Co., 16399 W. Bernardo Dr., San Diego, CA 92127, USA

BLAYNE M. MCKENZIE, Department of Macromolecular Science and Engineering, Case Western Reserve University, 2100 Adelbert Road, Cleveland, OH 44 106-7202, USA

D. TYLER MCQUADE, Department of Chemistry and Biochemistry, Florida State University, Tallahassee, FL 32306, USA

KAMLESH P. NAIR, School of Chemistry and Biochemistry, Georgia Institute of Technology, Atlanta, GA 30332-0400, USA

YUVAL OFIR, Department of Chemistry, University of Massachusetts, Amherst, 710 North Pleasant Street, Amherst, MA 01003, USA

JON R. PARQUETTE, Department of Chemistry, Ohio State University, 100 West 18th Avenue, Columbus, OH 43210, USA

STUART J. ROWAN, Department of Macromolecular Science and Engineering, Case Western Reserve University, 2100 Adelbert Road, Cleveland, OH 44106-7202, USA

HUI SHAO, Department of Chemistry, Ohio State University, 100 West 18th Avenue, Columbus, OH 43210, USA

KEN D. SHIMIZU, Department of Chemistry and Biochemistry, University of South Carolina, Columbia, SC 29208, USA

JEREMY L. STEINBACHER, Baker Laboratory, Department of Chemistry and Chemical Biology, Cornell University, Ithaca, NY 14853

RAYMOND J. THIBAUT, Epoxies Research and Development, The Dow Chemical Company, 2301 N Brazosport Blvd, Freeport, TX 77541-3257, USA

MARCUS WECK, Molecular Design Institute and Department of Chemistry, 100 Washington Square East, New York University, New York, NY 10003-6688, USA

XIANGYANG WU, University of South Carolina, Department of Chemistry and Biochemistry, Columbia, SC 29208, USA

VIRANY M. YUWONO, Department of Chemistry, Rice University, Mail Stop 60, 6100 Main Street, Houston, TX 77005, USA

## LIST OF FIGURES

---

**Figure 1.1** (a) Supramolecular polymers developed by Lehn using three-point hydrogen bonds between diamidopyridine and thymine residues and (b) analogous polymers by Meijer employing self-complementary, quadruple hydrogen bonds. (c) A schematic depiction of the extended chain of repeating bisfunctional monomers forming the backbone of supramolecular polymers.

**Figure 1.2** A schematic representation of the versatility of reversible, supramolecular side-chain modification and selected examples of interactions that can be employed.

**Figure 2.1** Representation of different types of copolymers.

**Figure 2.2** Representation of formation of (a) micellar and (b) inverse micellar vesicular assemblies from diblock and triblock copolymers, respectively.

**Figure 2.3** Representation of organized assemblies (a) bilayers, (b) cylindrical micelles, and (c) lamellar structure.

**Figure 2.4** Temperature responsive micellar formation in PNIPAM-based polymers.

**Figure 2.5** Formation of micellar assemblies induced by pH complexation in ionic block copolymers.

**Figure 2.6** Schematic representation of the formation of micelle and rodlike structures of amphiphilic conjugate of oligonucleotide and PPO.

**Figure 2.7** Formation of micellar and inverted micellar assemblies from amphiphilic homopolymer.

**Figure 2.8** Interaction of anionic amphiphilic homopolymeric micelle with the positive patch of protein.

**Figure 2.9** Interaction of polymeric micelles that contain anthracene units (a) with nonmetalloproteins and (b) with metalloproteins.

**Figure 2.10** Selective extraction of peptides utilizing amphiphilic homopolymeric micelles.

**Figure 3.1** Quadruple hydrogen-bonded 2-ureido-4-pyrimidinone units attached to the ends of a polydimethylsiloxane chain assemble to create materials with viscoelastic properties.

**Figure 3.2** A mechanical force causes a loss of an entanglement in a covalent polymeric network by one of two major mechanisms: process A, chain slippage via reptation; process B, chain scission.

**Figure 3.3** Entanglement response to a mechanical force in a supramolecular system: process A, chain slippage via reptation; process B, chain scission via breaking of the supramolecular bond.

**Figure 3.4** Relationship between the equilibrium association constant ( $K_{eq}$ ) and the rate constants for supramolecular association and dissociation.

**Figure 3.5** Pincer-ligand motifs that provide independent control of supramolecular association/dissociation kinetics relative to thermodynamics.

**Figure 3.6** Schematic of a supramolecular polymer network.

**Figure 3.7** (a) Storage modulus versus frequency for the networks **5** · PVP and (b) the same storage modulus scaled by  $k_{diss}$  of model complexes **1** · **2a** versus the frequency of oscillation scaled by the same  $k_{diss}$ . Each of the networks consists of 5% (by metal functional group per pyridine residue) of (●) **5a**, (▲) **5b**, (■) **5c**, and (◆) **5d** and PVP at 10% by total weight of the network in DMSO at 20°C. Data taken from Loveless et al. (2005).

**Figure 3.8** Dynamic viscosity versus frequency for (●) 2.5% + 2.5% (**5b** + **5c**) · PVP, (□) 2.5% **5c** · PVP, (△) 5% **5c** · PVP, (+) 2.5% **5b** · PVP, and (×) 5% **5b** · PVP. All networks are 10% by total weight in DMSO at 20 °C. Data taken from Loveless et al. (2005).

**Figure 3.9** Supramolecular bridges between two surfaces.

**Figure 3.10** Reversible base pairing defines the rigid structure of a reversible polymer system.

**Figure 3.11** Poly(4-vinylpyridine) brushes subsequently exposed to metallic cross-linkers. The addition of **4a** decreases the lateral friction, but the addition of **4b** increases the lateral friction.

**Figure 4.1** Degree of noncovalent polymerization as a function of the association constant ( $K_a$ ). The effect of concentration is illustrated in the two parallel

lines. Reprinted from Brunsveld et al. (2001). Copyright 2001 American Chemical Society.

**Figure 4.2** An Archimedean tile morphology for blends of poly(2-vinylpyridine-*b*-isoprene-*b*-vinylpyridine) with poly(styrene-*b*-4-hydroxystyrene) in a 2:1 vinylpyridine/hydroxystyrene blend. The vinylpyridine/hydroxystyrene domains are the cylinders at the vertices of polystyrene hexagons within a polyisoprene continuous phase. Reprinted from Asari et al. (2006). Copyright 2006 American Chemical Society.

**Figure 4.3** Synthesis of adenine containing block copolymers via a ROMP methodology. Reprinted from Bazzi and Sleiman (2002). Copyright 2002 American Chemical Society.

**Figure 4.4** Formation of cylindrical aggregates via multidirectional self-association bonding of adenine functional block copolymers. Reprinted from Bazzi and Sleiman (2002). Copyright 2002 American Chemical Society.

**Figure 4.5** Scheme for stepwise synthesis of oligonucleotides via coupling of phosphoramidite-functionalized nucleosides. Reprinted from Noro et al. (2005). Copyright 2005 American Chemical Society.

**Figure 4.6** Phosphoramidite coupling onto hydroxyl-functionalized ROMP polymers (Watson et al. 2001).

**Figure 4.7** Synthesis of PNA-functionalized crosslinker molecule and association of a complementary PNA-terminated polymer synthesized by ATRP (Wang et al. 2005).

**Figure 4.8** Synthesis of dicarboximide functional hydrogen bonding block copolymers via ROMP (Dalphon d et al. 2002).

**Figure 4.9** Hydrogen bonding attachment of flavin to diaminotriazine-functional polystyrene (Deans et al. 1999).

**Figure 4.10** Hydrogen bonding block codendrimer synthesized by Yuan et al. (2006).

**Figure 4.11** Solution viscosity of (a) telechelic UPy functional poly(dimethylsiloxane) and (b) a benzyl protected analog in chloroform at 20 °C. Reprinted from Cates (1987). Copyright 1987 American Chemical Society.

**Figure 4.12** Tautomeric equilibrium of UPy dimer with Napy-UPy heterodimer (Scherman et al. 2006).

**Figure 4.13** Compatibilization of poly(ether ketone) with poly(isobutylene) using Janus wedge hydrogen bonding (Binder et al. 2005).

**Figure 4.14** Calixarene synthesized by Castellano et al. (2000). Reprinted from Castellano et al. (2000). Copyright 2000 National Academy of Sciences USA.

**Figure 4.15** Dual side chain noncovalent interaction modes including both hydrogen bonding and metal–ligand interactions. Reprinted from Nair et al. (2006). Copyright 2006 American Chemical Society.

**Figure 4.16** Phase diagram of poly(isoprene-*b*-2-vinylpyridine) with octyl gallate, indicating the transition between different morphologies with octyl gallate content and temperature (D, disordered; S, spherical; H, hexagonal; L, lamellar; L2, lamellar with reduced spacing; I, intermediate state). Reprinted from Bondzic et al. (2004). Copyright 2004 American Chemical Society.

**Figure 5.1** Examples of hydrogen bonding motifs used in side chain functionalizations of polymers: (a) one-point complementary, (b, c) two-point dimerizing, (d, e) three-point complementary, (f) four-point dimerizing, (g) four-point complementary, and (h) six-point complementary hydrogen bonding motifs.

**Figure 5.2** Examples of hydrogen bonding motifs used in supramolecular polymers: dimerizing ureidopyrimidone (UPy) functionalized main chain supramolecular polymers (**2A**), simple one-point complementary hydrogen bonding interactions between pyridine and phenol (**2B**), and six-point complementary hydrogen bonding interaction between cyanuric acid and the Hamilton wedge receptor (**2C**).

**Figure 5.3** Examples of metal coordination motifs employed for side chain functionalization of polymers.

**Figure 5.4** Examples of charged coulombic moieties employed for side chain functionalization of polymers.

**Figure 5.5** Side chain functionalization of diblock copolymers **1** and **2**, using a combination of hydrogen bonding and metal coordination.

**Figure 5.6** Functionalization strategies of random copolymer **3** based on a combination of hydrogen bonding and coulombic interactions.

**Figure 5.7** Functionalization strategies of copolymer **4** based on multiple hydrogen bonding interactions.

**Figure 5.8** Three recognition motifs based on (a) hydrogen bonding interactions between 2,6-diaminopyridine and thymine, (b) metal coordination of sulfur–carbon–sulfur (SCS) Pd pincer with pyridine, (c) pseudorotaxane formation between dibenzo[24]*crown*-8 (DB24C8) and dibenzylammonium ions, and (d) fully functionalized terpolymer **5**.

**Figure 5.9** Examples of supramolecular side chain liquid crystalline polymers (SSCLCPs) based on hydrogen bonding (**6** and **7**) and coulombic interactions and hydrogen bonding (**8**).

**Figure 5.10** Diverse applications using hydrogen bonding interactions employed by Rotello and coworkers (Arumugam et al. 2007): (a) self-assembled dendronized polymer and (b) inorganic–organic hybrid material using barbiturate functionalized nanoparticles and Hamilton wedge functionalized block copolymers.

**Figure 5.11** The three distinct classes of hydrogen bonded polymer networks: (a) self-associative polymer network, (b) polymer network synthesized via the use of complementary linker molecules, and (c) complementary polymer blends.

**Figure 5.12** Self-associative hydrogen bonded polymer networks based on (a) 2-ureido-4[1H]-pyrimidone (UPy), (b) 1,2,4-triazine, and (c) urazole carboxylic acid.

**Figure 5.13** Self-associative polymer network formed via the dimerization of 2-ureido-4[1H]-pyrimidone groups attached to the polymer backbone.

**Figure 5.14** Schematic representation of polymer network formation based on the addition of complementary linkers using (a) single hydrogen bond formation and bifunctional cross-linking agents, (b) single hydrogen bond formation and trifunctional cross-linking agents, and (c) three-point hydrogen bond formation and bifunctional cross-linking agents.

**Figure 5.15** Examples of linker cross-linked polymer networks exhibiting liquid crystalline polymer characteristics.

**Figure 5.16** 2,6-Diaminopyridine side chain functionalized polystyrene cross-linked via bis-thymine cross-linking agents.

**Figure 5.17** Noncovalent cross-linking strategies of cyanuric acid functionalized poly-CA to form (a) poly-CA-triazine by using a diaminotriazine cross-linking agent or (b) poly-CA-wedge by using an isophthalamide cross-linking agent.

**Figure 5.18** Cross-linking profile of poly-CA using the triazine-based cross-linking agent. Filled symbols denote the elastic modulus ( $G'$ ) whereas empty symbols denote the loss modulus ( $G''$ ) at a strain value of 0.1. The percentage of the triazine-based cross-linking agent is based on the cyanuric acid groups attached to the polymer.

**Figure 5.19** Homogenous polymer blend of 2,7-diamido-1,8-naphthyridine (DAN) functionalized polystyrene and urea of guanosine (UG) functionalized poly(butyl methacrylate) (**14**), based on the four-point complementary complex formation between DAN and UG.

**Figure 5.20** Examples of metal cross-linked polymer networks.

**Figure 5.21** Orthogonal noncovalent cross-linking as well as functionalization strategy of terpolymer using hydrogen bonding and metal coordination interactions.

**Figure 6.1** General schematic representation of polymer-mediated assembly of nanoparticles: (a) functionalization of nanoparticles through place-exchange method, (b) incorporation of complementary functional group to polymers, and (c) self-assembly of nanoparticles through electrostatic or hydrogen bonding interactions.

**Figure 6.2** (a) Gold nanoparticles assembled using PAMAM dendrimers and (b) small angle X-ray scattering (SAXS) plots of nanoparticle assembly indicating systematic control of interparticle distance by dendrimer generations. Reprinted with permission from Frankamp, Boal, et al. (2002). Copyright 2002 American Chemical Society.



**Figure 6.3** UV visible spectra of assembled gold nanoparticle thin films by dendrimers of different generations ranging from G0 to G4. Reprinted with permission from Srivastava, Frankamp, et al. (2005). Copyright 2005 American Chemical Society.

**Figure 6.4** (a) Self-assembly of magnetic FePt nanoparticles by DNAs and (b) a TEM micrograph of network-like FePt–DNA aggregates; scale bar = 100 nm. Reprinted with permission from Srivastava, Samanta, Arumugam, et al. (2007). Copyright 2007 RSC Publishing.

**Figure 6.5** (a) The formation of ferritin-mediated self-assembly of FePt nanoparticles via electrostatic interactions, (b) magnetic dipole–dipole interaction of ferritins assembled with FePt nanoparticles, and (c) zero field cooling and field cooling results for the ferritin–FePt nanoparticle composite film and individual components. Reprinted with permission from Srivastava, Samanta, Jordan, et al. (2007). Copyright 2007 American Chemical Society.

**Figure 6.6** (a) Schematic representation of PEI-mediated assembly of gold nanoparticles. Transmission electron micrographs of (b) hexagonal and (c) cubic packing arrangements of nanoparticles. Reprinted with permission from Schmid et al. (2000). Copyright 2000 Wiley InterScience.

**Figure 6.7** Illustration of multipoint hydrogen bonding based self-assembly: (a) hydrogen bond formation between barbituric acid functionalized gold nanoparticles and Hamilton receptor functionalized block copolymers and (b) selective deposition of nanoparticles on a microphase-separated block copolymer film. Reprinted with permission from Binder et al. (2005). Copyright 2005 American Chemical Society.

**Figure 6.8** TEM micrographs of (a) “dots” patterned samples formed through affinity of Terpy-functionalized gold nanoparticles on PS domain, (b) Fe-treated cross-linked samples, and (c) ethanol-treated samples after swelling in chloroform vapor. Reprinted with permission from Shenhar et al. (2005). Copyright 2005 Wiley InterScience.

**Figure 6.9** A schematic representation of orthogonal process for nanoparticles self-assembly: (a) a patterned silicon wafer with Thy-PS and PVMP polymers fabricated through photolithography and (b) orthogonal surface functionalization through Thy-PS/DP-PS recognition and PVMP/acid–nanoparticle electrostatic interaction. Reprinted with permission from Xu et al. (2006). Copyright 2006 American Chemical Society.

**Figure 6.10** A procedural schematic representation for deposition of two kinds of particle arrays on the patterned template. Reprinted with permission from Zheng et al. (2002). Copyright 2002 Wiley InterScience.

**Figure 6.11** (a) Scheme of patterning nanoparticle thin films and (b) scanning electron micrograph of self-assembly patterns after lift-off process. Reprinted with permission from Hua et al. (2002). Copyright 2002 American Chemical Society.